

# Quantum melting of the quasi-two-dimensional vortex lattice in $\kappa$ -(ET)<sub>2</sub>Cu(NCS)<sub>2</sub>

M. M. Mola and S. Hill<sup>†</sup>

*Department of Physics, Montana State University, Bozeman, MT 59717*

J. S. Brooks and J. S. Qualls

*Department of Physics and National High Magnetic Field Laboratory, Florida State University, Tallahassee, FL 32310*

(February 1, 2008)

We report torque magnetization measurements in regions of the mixed state phase diagram ( $\mathbf{B} \sim \mu_o \mathbf{H}_{c2}$  and  $T_c/10^3$ ) of the organic superconductor  $\kappa$ -(ET)<sub>2</sub>Cu(NCS)<sub>2</sub> where quantum fluctuations are expected to dominate thermal effects. Over most of the field range below the irreversibility line ( $\mathbf{B}_{irr}$ ), magneto-thermal instabilities are observed in the form of flux jumps. The abrupt cessation of these instabilities just below  $\mathbf{B}_{irr}$  indicates a quantum melting transition from a quasi-two-dimensional vortex lattice phase to a quantum liquid phase.

PACS numbers: 74.70.Kn, 74.60.Ec, 74.60.Ge, 74.25.Ha

Although the properties of vortices in layered type-II superconductors have been studied vigorously for over 15 years, this subject continues to provide a rich and varied field for investigation. The mixed superconducting state represents a wonderful playground for studying general phase transformations associated with vortex matter [1]. In particular, melting of the Abrikosov vortex lattice into a liquid phase has drawn considerable interest, especially in extreme type-II superconductors such as the high temperature superconductors [2] (HTS) and organic superconductors [3]. Moreover, identification of a melting transition driven by quantum (as opposed to thermal) fluctuations has drawn much attention, both theoretically [4] as well as experimentally [5]. A thorough understanding of vortex physics is also essential for determining possible limiting behavior for technological applications utilizing superconductors.

A model system for investigation of the structure and dynamics of vortices in layered, type-II, superconductors is  $\kappa$ -(ET)<sub>2</sub>Cu(NCS)<sub>2</sub>, where ET denotes bis-ethylenedithio-tetrathiafulvalene [6]. Like the HTS, this organic superconductor possesses a highly anisotropic layered structure with the superconducting ET planes separated by insulating anion layers [6]. The anisotropy parameter,  $\gamma$ , defined as the ratio of the interlayer (currents  $\parallel$   $a$ -axis) and in-plane (currents  $\parallel$   $bc$ -plane) penetration depths ( $\gamma \equiv \lambda_a/\lambda_{bc}$ ), is thought to be in the range 50-200 [7], *i.e.* similar to that of Bi<sub>2</sub>Sr<sub>2</sub>CaCu<sub>2</sub>O<sub>8+d</sub> [8]. Consequently, in comparison to conventional superconductors, fluctuation effects may be expected to play an important role at low-temperatures. In contrast to the HTS, the organic superconductors are extremely clean, with very few crystal defects. Furthermore, because of the reduced  $T_c$  and  $\mathbf{H}_{c2}$  ( $T_c = 9 - 10$  K [6,9,10] and  $\mu_o \mathbf{H}_{c2} \approx 5$  T (30 - 35 T) [9,10] for the field perpendicular (parallel) to the superconducting layers), one is able to probe much more of the temperature/field parameter space within the superconducting state than is currently

possible in the HTS. This, in turn, raises the interesting prospect of studying two dimensional vortex lattice melting over an extended temperature range (from  $T_c$  to  $T_c/10^3$ ) - possibly into the (low T, high  $\mathbf{B}$ ) quantum regime. Magnetic relaxation measurements performed by Mota *et al.* [11], have shown that the crossover temperature from thermal to quantum dominated fluctuations occurs at around 0.5 K for this material.

It is well known from muon spin rotation ( $\mu$ SR) measurements that a three-dimensional (3D) flux line lattice exists only at very low fields ( $< 7$  mT  $\ll \mu_o \mathbf{H}_{c2}$ ) in the title compound [12]; due to the large  $\gamma$  value, the individual quasi-two-dimensional (Q2D) vortex lattices in adjacent layers become effectively decoupled above a roughly temperature independent dimensional crossover field  $\mathbf{B}_{cr}$  ( $\sim 7$  mT, see Fig. 1 and Ref. [12]). Our recent temperature dependent investigations of the interlayer Josephson plasma resonance (JPR) in  $\kappa$ -(ET)<sub>2</sub>Cu(NCS)<sub>2</sub> provide conclusive proof that, in spite of the decoupling, long range Q2D order among vortices within individual layers persists over most of the region in the phase diagram between  $\mathbf{B}_{cr}$  and the irreversibility line (see shaded region in Fig. 1 and Refs [13,14]). Immediately below the irreversibility line, local magnetization measurements [3], as well as the JPR studies [13], indicate a transition in this Q2D vortex structure (see Fig. 1) - Q2D melting has been put forward as one possible explanation for this transition [3,13]. These findings serve as a motivation for investigating a wider range of the  $\mathbf{B}, T$  phase diagram.

High quality single crystals were grown using standard techniques [6]. A single sample (approximate dimensions  $1.0 \times 1.0 \times 0.3$  mm<sup>3</sup>) was mounted on a capacitive cantilever beam torque magnetometer which, in turn, was attached to a single axis rotator;  $\theta = 0^\circ$  corresponds to the field parallel to the least conducting  $a$ -axis, while  $\theta = 90^\circ$  corresponds to the field parallel to the highly conducting  $bc$ -planes. The sample, cantilever and rotator were then loaded directly into the mixing chamber

of a top-loading  $^3\text{He}/^4\text{He}$  dilution refrigerator situated within the bore of a 20 T superconducting magnet at the National High Magnetic Field Laboratory (NHMFL). For all measurements reported here, the magnetic field was swept at a constant rate of 0.5 T/min. Temperature dependent torque measurements were performed at  $\theta = 47^\circ$  and  $74^\circ$ . Subsequent analysis of the angle dependence (from  $\theta = 0^\circ$  to  $90^\circ$ ) enabled us to scale the temperature dependence back to  $\theta = 0^\circ$ , where the torque is zero in this setup.

In Fig. 2, we plot the magnetization  $\mathbf{M}$ , derived directly from the torque  $\tau$  ( $\mathbf{M} = \tau/\mathbf{B}\sin\theta$ ), as a function of the applied magnetic field strength  $\mathbf{B}$ , for angles between  $\theta \sim 30^\circ$  and  $79^\circ$  at approximately  $10^\circ$  intervals; the temperature is 25 mK. The overall shape of these curves is consistent with previous measurements [15,16]. The observed magnetization and associated hysteresis (arrows in Fig. 2 indicate the field sweep direction) are a consequence of the viscous flow of magnetic flux into (out of) the sample upon increasing (decreasing) the applied magnetic field strength. The hysteresis is greatest at low fields, and can be seen to disappear completely above a characteristic field  $\mathbf{B}_{irr}$  ( $< \mu_o\mathbf{H}_{c2}$ ), above which the sample behaves reversibly. Perhaps the most pronounced features of the data in Fig. 2 are the abrupt magnetization jumps. These "flux jumps" have been observed previously in this and other materials [16,17,18], and are due to an avalanche behavior associated with the reorganization of magnetic flux as it enters the sample; a systematic analysis of this phenomenon can be found in Ref. [19].

In the region between  $\mathbf{B}_{cr}$  and  $\mathbf{B}_{irr}$ , crystal defects collectively pin the Q2D vortex lattices in each layer. Thus, in a field swept experiment, there is a build up of flux near the sample surface. This creates a field gradient at the sample edge together with an associated surface current given simply by Maxwell's equation:  $\nabla \times \mathbf{B} = \mu_o\mathbf{J}_c$ , where  $\mathbf{J}_c$  is the in-plane critical current density [20,21]. At extremely low temperatures, a thermal boundary (Kapitza) resistance [22] isolates the sample from the surrounding cryogen bath. Viscous transport of vortices across the sample edge (where the surface screening currents flow) causes local heating which, in turn, reduces the critical current density, leading to additional heating and so on.. In the absence of an effective thermal link to the surroundings, this can result in runaway thermal instabilities which cause macroscopic regions of the sample to become metallic [18,23]. When this occurs, flux is able to flow rapidly into the crystal's interior, thereby negating any/most of the surface currents. The crystal then quickly cools and once again becomes superconducting with a slightly different metastable vortex arrangement; the process then starts anew. Indeed, Legrand *et al.* [18], have shown that, for a field swept experiment,  $\text{YBa}_2\text{Cu}_3\text{O}_7$  samples experience large temperature spikes in conjunction with discontinuities in the magnetization. These jumps are then followed

by a rapid relaxation back to the surrounding bath temperature, consistent with the model above. An analysis of the temperature dependence of the magnitudes of the observed magnetization jumps ( $\propto T^{3/2}$ ) in Fig. 2 supports this picture – see Ref. [19]. An important consequence of this model is that the observation of flux jumps depends on the stiffness of the vortex structure, *i.e.* jumps will only be observed when collective vortex pinning is strong. These flux jumps can thus be used as an indication of the existence of a vortex solid of some sort.

In Fig. 3 we plot close-ups of the (raw) data in Fig. 2 in the vicinity of  $\mathbf{B}_{irr}$ . Notice that, for small angles (Fig. 3a), there is a noticeable kink in the magnetization at an angle dependent field, denoted  $\mathbf{B}_m$  (indicated by arrows), just slightly below  $\mathbf{B}_{irr}$ . Prior to this kink, the flux jumps decay – becoming negligibly small in the vicinity of the kink – while, above the kink, the magnetization decreases smoothly to the reversible domain. At larger angles (Fig. 3b), flux jumps persist up to the kink, but never beyond. In fact, at the largest angles, the amplitudes of the flux jumps are very large – much larger than the kink amplitude – and, thus, the kink is not discernible. However, an abrupt cessation of the flux jumps is instead observed at a field whose angle dependence merges smoothly into the angle dependence of the kink field  $\mathbf{B}_m$  (see Fig. 4a). Thus, we assume that the dramatic flux jump cessation, and the kink observed at smaller angles, are related. The fact that the flux jumps cease at  $\mathbf{B}_m$  suggests that the stiffness of the vortex system changes – possibly due to a melting transition (see below). In what follows, we identify  $\mathbf{B}_m$  by the kink at low angles, and the flux jump cessation at high angles.

In Fig. 4a, we have plotted  $\mathbf{B}_m$  and  $\mathbf{B}_{irr}$  vs.  $\theta$ . The solid lines are fits to the data using the following scaling law derived from 2D Ginzburg-Landau theory [10]:

$$\left| \frac{\mathbf{B}_c(\theta)\sin\theta}{\mathbf{B}_{c\perp}} \right| + \left( \frac{\mathbf{B}_c(\theta)\cos\theta}{\mathbf{B}_{c\parallel}} \right)^2 = 1,$$

where  $\mathbf{B}_c$  refers to either  $\mathbf{B}_m$  or  $\mathbf{B}_{irr}$ , and the subscripts  $\parallel$  and  $\perp$  refer to the limiting values of these fields with  $\theta = 90^\circ$  and  $\theta = 0^\circ$ , respectively; the same angle dependence has also been noted for  $\mathbf{H}_{c2}$  [10]. From the fit to  $\mathbf{B}_m(\theta)$ , we obtain values for  $\mathbf{B}_{m\perp} = 3.6$  T and  $\mathbf{B}_{m\parallel} = 32$  T, at  $T = 25$  mK. Thus,  $\mathbf{B}_m(\theta)$  falls below  $\mathbf{B}_{irr}$ , and well below  $\mu_o\mathbf{H}_{c2}$  – a region in  $\mathbf{B},T$  parameter space where no such transition has previously been observed (earlier low-temperature experiments measured only  $\mathbf{B}_{irr}$  [16]). Using two separate models [4,5], Sasaki *et al.* [16], have made a rough estimate of the  $T = 0$  K,  $\theta = 0^\circ$  quantum melting field  $\mathbf{B}_{qm\perp}$  for  $\kappa\text{-(ET)}_2\text{Cu(NCS)}_2$ . For either model, they obtain  $\mathbf{B}_{qm\perp} \sim 4$  T, very close to the transition field  $\mathbf{B}_{m\perp}$  we observe at 25mK. Thus, given the extremely low temperature of these measurements

( $T \sim T_c/10^3$ ), along with the proximity to the expected  $T = 0$  K quantum melting field, we propose that the observed transition at  $\mathbf{B}_m(\theta, T < 200\text{mK})$  does in fact correspond to a quantum melting transition between a Q2D vortex lattice phase and a quantum liquid phase. The existence of a liquid phase dominated by quantum fluctuation effects in the region between  $\mathbf{B}_{irr}$  and  $\mu_o\mathbf{H}_{c2}$  has, indeed, been noted by other authors [16,24].

The temperature dependence of  $\mathbf{B}_m$  provides further evidence that quantum effects become important as  $T \rightarrow 0$  K. After scaling measurements made at  $\theta = 47^\circ$  back to  $\theta = 0^\circ$ , we plot  $\mathbf{B}_m$  and  $\mathbf{B}_{irr}$  as a function of temperature in Fig. 4b. In this  $\mathbf{B}, T$  regime, the irreversibility line shows a linear temperature dependence, consistent with previous measurements [16], while  $\mathbf{B}_m$  exhibits a definite negative curvature [ $\mathbf{B}_m \propto (T_c - T)^\alpha$ ,  $\alpha < 1$ ]; no classical theory of melting can account for this trend. Nevertheless, Blatter *et al.* have observed a similar behavior in 2D superconducting films, which they attribute to a crossover from quantum melting to a thermally assisted dislocation mediated form of melting at higher temperatures [5]. The crossover temperature predicted by Blatter *et al.* occurs at around  $T \sim T_c/100$ , which is precisely where we observe the negative curvature (or crossover) in the temperature dependence of  $\mathbf{B}_m$ . Clearly, measurements spanning a wider temperature range will be necessary in order to elucidate the true nature of the melting at higher temperatures. However, the fact that the phase boundary curves directly towards the  $T = 0$  K axis, as  $T \rightarrow 0$  K, is strongly suggestive of a quantum phase transition.

Measurements on a second larger sample produced similar flux jumps [25], and exactly the same abrupt flux jump cessation just below  $\mathbf{B}_{irr}$ , as seen in Fig 3b. In fact, a data point for this second sample falls precisely on the melting curve in Fig 4a. Although the flux jumps are sample dependent [25], their cessation appears to be sample independent, indicating that the supposed melting transition is intrinsic, *i.e.*  $\mathbf{B}_m(T, \theta)$  is unaffected by sample shape, size, or details of the sample's surface.

The pronounced hysteresis in  $\mathbf{B}_m$  could be taken as an indication of 1<sup>st</sup> order behavior, as could the kink in  $\mathbf{M}$  observed at  $\mathbf{B}_m$ ; note that, for several traces in Fig. 3a, the kink has the appearance of a discontinuous jump. However, it is difficult truly judge the order of the transition based on the hysteresis, given the many factors which contribute to asymmetry in the  $\mathbf{M}$  vs.  $\mu_o\mathbf{H}$  loops. Indeed, these factors may lead to physically different transitions on up and down sweeps. The approach from low fields is preceded by frequent catastrophic 1<sup>st</sup> order flux avalanches and temperature spikes. Thus, disorder and/or dislocations could play a role in the up-sweep melting, though the extreme quality of these samples would seemingly rule out plastic or glassy behavior (our JPR studies have shown the pinning in this material to be several orders of magnitude weaker than in the HTS

[13]). The approach from high fields, on the other hand, simply involves a transition from a weakly pinned liquid state [1] to the ordered state. These matters aside, we assert that it is the abrupt cessation of flux jumps at  $\mathbf{B}_m$ , together with the angle dependence of  $\mathbf{B}_m$ , that suggest a 2D melting transition. From the temperature dependence of  $\mathbf{B}_m$ , we additionally propose that the melting transition becomes 1<sup>st</sup> order, and is driven by quantum fluctuations as  $T \rightarrow 0$ .

Taking this new high field/low temperature data, and combining it with previous JPR [13], local magnetization [3,16], and  $\mu\text{SR}$  [12] measurements, we can construct a mixed state phase diagram for  $\kappa\text{-(ET)}_2\text{Cu(NCS)}_2$ , as shown in Fig. 1. It is tempting to connect the present data to the data from Refs. [3] and [13] with a smooth curve (see dashed line in Fig. 1). This would seem to suggest that both transitions correspond to Q2D melting. We should note, however, that the high temperature phase line may be due to a thermally assisted depinning transition, as noted in Ref. [13]. Finally, the present measurements have been unable to detect any indication of the transition to a Fulde-Ferrell-Larkin-Ovchinnikov state reported recently by Singleton *et al.* close to  $\theta = 90^\circ$  [26].

In conclusion, we have observed magneto-thermal instabilities in the mixed state of the organic superconductor  $\kappa\text{-(ET)}_2\text{Cu(NCS)}_2$ , which are associated with transitions between metastable Q2D vortex lattice phases. The abrupt cessation of magnetization jumps associated with these instabilities serve as an indication of a melting of this Q2D vortex lattice phase. Furthermore, this study – which is the first of its kind in the high- $\mathbf{B}$ /low- $T$  limit for such a highly anisotropic superconductor – suggests that the melting may be driven by quantum rather than thermal fluctuations. Future investigations will focus on the temperature dependence of this transition, and on its evolution away from the high- $\mathbf{B}$ /low- $T$  limit.

This work was supported by the National Science Foundation (DMR-0071953) and the Office of Naval Research (N00014-98-1-0538). Work carried out at the NHMFL was supported by a cooperative agreement between the State of Florida and the NSF under DMR-9527035.

---

† email: hill@physics.montana.edu

- [1] G. Blatter *et al.*, Rev. Mod. Phys. **66**, 1125 (1995).
- [2] See G. W. Crabtree and D. R. Nelson, Physics Today **50**, 38 (AIP, April 1997); and references therein.
- [3] M. Inada *et al.*, J. Low Temp. Phys. **117**, 1423 (1999); and references therein.

- [4] A. Rozhkov and D. Stroud, Phys. Rev. B **54**, R12697 (1996).
- [5] G. Blatter *et al.*, Phys. Rev. B **50**, 13013 (1994).
- [6] T. Ishiguro, K. Yamaji, and G. Saito, *Organic Superconductors* (Springer-Verlag, Berlin, 1998).
- [7] A. Carrington *et al.*, Phys. Rev. Lett. **83**, 4172 (1999); and references therein.
- [8] Y. Matsuda *et al.*, Phys. Rev. Lett. **78**, 1972 (1997).
- [9] M. Lang *et al.*, Phys. Rev. B **49**, 15227 (1994).
- [10] F. Zuo *et al.*, Phys. Rev. B **61**, 750 (2000); and references therein.
- [11] A. C. Mota *et al.*, Physica C **185-189**, 343 (1991).
- [12] S. L. Lee *et al.*, Phys. Rev. Lett. **79**, 1563 (1997); F. L. Pratt *et al.*, submitted.
- [13] M. M. Mola *et al.*, Phys. Rev. B **62**, (2000).
- [14] The only theoretical models that can account for the temperature dependence observed in Ref. [13] assume pinned Q2D solid vortex lattices in each layer, with no correlation between the locations of vortices in adjacent layers.
- [15] T. Nishizaki *et al.*, Phys. Rev. B **54**, R3760 (1996).
- [16] T. Sasaki *et al.*, Phys. Rev. B **57**, 10889 (1998).
- [17] A. G. Swanson *et al.*, Solid State Comm. **73**, 353 (1990).
- [18] L. Legrand *et al.*, Physica C **211**, 239 (1993).
- [19] M. Mola *et al.*, cond-mat/0011227.
- [20] D. R. Tilley and J. Tilley, *Superfluidity and Superconductivity* (IOP Publishing, London, 1990).
- [21] C. P. Bean, Rev. Mod. Phys. **36**, 31 (1964).
- [22] A. Kent, *Experimental Low-Temperature Physics* (AIP, New York, 1993).
- [23] R. G. Mints and A. L. Rakhmanov, Rev. Mod. Phys. **53**, 551 (1981).
- [24] H. Ito *et al.*, J. Superconductivity **12**, 525 (1999).
- [25] Limited data were obtained for this second sample due to the fact that its larger magnetic moment overwhelmed the detection scheme of the magnetometer.
- [26] J. Singleton *et al.*, J. Phys.: Condens. Matter **12**, L641 (2000).

## Figure captions

Fig. 1. The mixed state **B,T** phase diagram for  $\kappa$ -(ET)<sub>2</sub>Cu(NCS)<sub>2</sub>. The legends correspond to:  $\diamond$  –  $\mu_o\mathbf{H}_{c2}$  [9];  $\nabla$  –  $\mathbf{B}_{irr}$  [16];  $\bullet$  – 2D melting or depinning [13];  $\square$  – first-order transition [3];  $\triangle$  – 3D to 2D crossover [12];  $\circ$  – 2D melting (this study). Note that the Q2D solid (shaded region) and liquid phases occupy most of the available **B,T**-space.

Fig. 2. Magnetization as a function of magnetic field (up- and down-sweeps) for angles  $\theta$  between  $\sim 30^\circ$  and  $79^\circ$ ; the temperature is 25 mK.

Fig. 3. Magnetization vs. magnetic field at (a) low and (b) high angles  $\theta$  (indicated in the figure). In (a), a distinct kink may be observed in the magnetization (indicated by arrows) at a field  $\mathbf{B}_m$  just below  $\mathbf{B}_{irr}$ ; the flux jumps decay smoothly to zero just before  $\mathbf{B}_m$ . At higher angles (b), the kink at  $\mathbf{B}_m$  is obscured by large amplitude flux jumps. However, the abrupt cessation of these flux jumps serves as an alternative indication of the phase transition.

Fig. 4. (a) Angle dependence of the melting and irreversibility fields,  $\mathbf{B}_m(\theta)$  and  $\mathbf{B}_{irr}(\theta)$  respectively; the solid lines are fits to the scaling law in Eq. 1. (b) Temperature dependence of the melting and irreversibility fields.

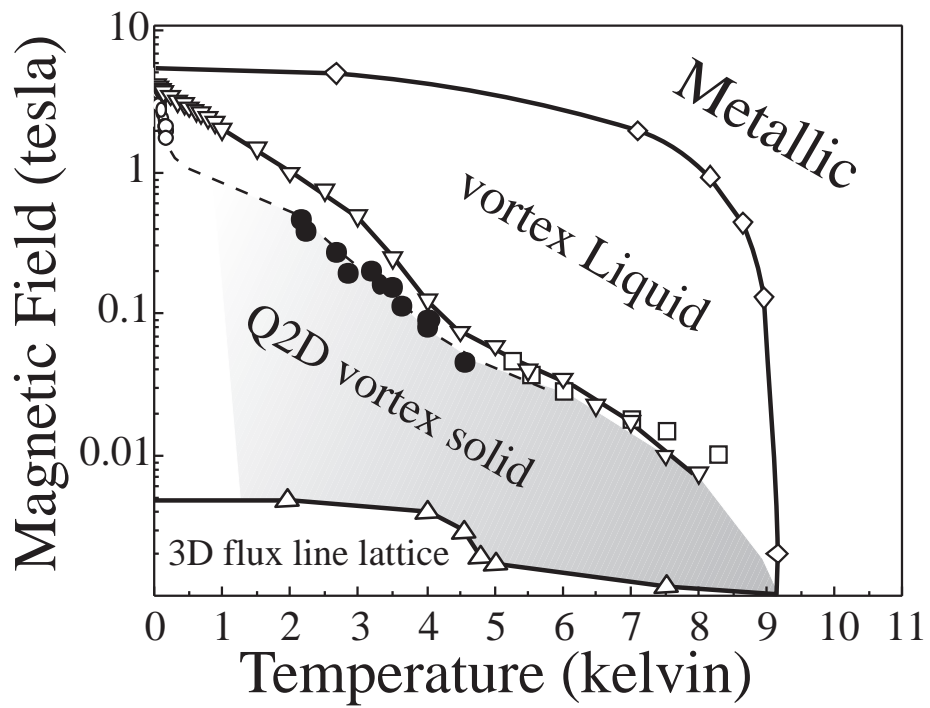


FIG. 1. Mola *et al.*

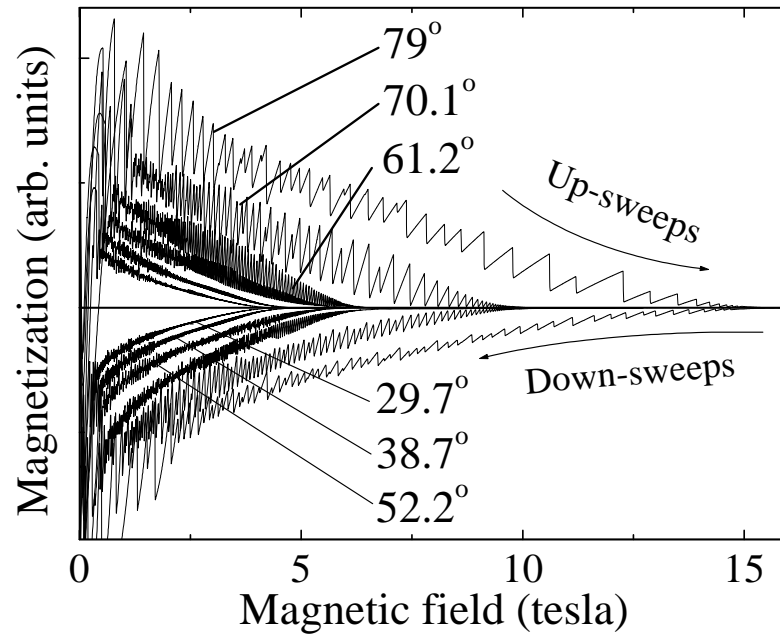


FIG. 2. Mola *et al.*

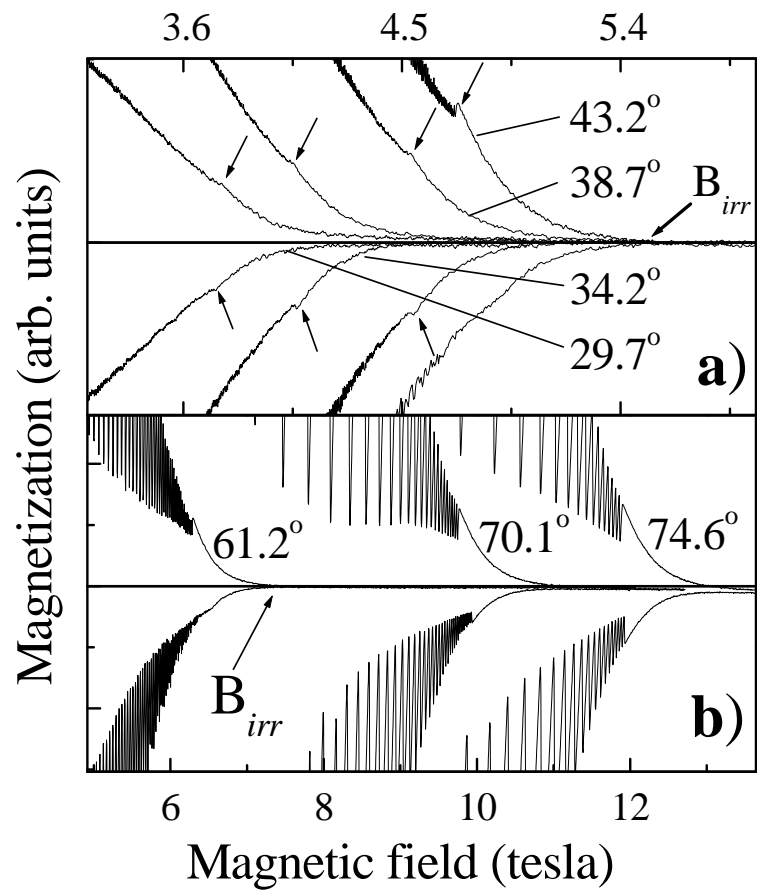


FIG. 3. Mola *et al.*

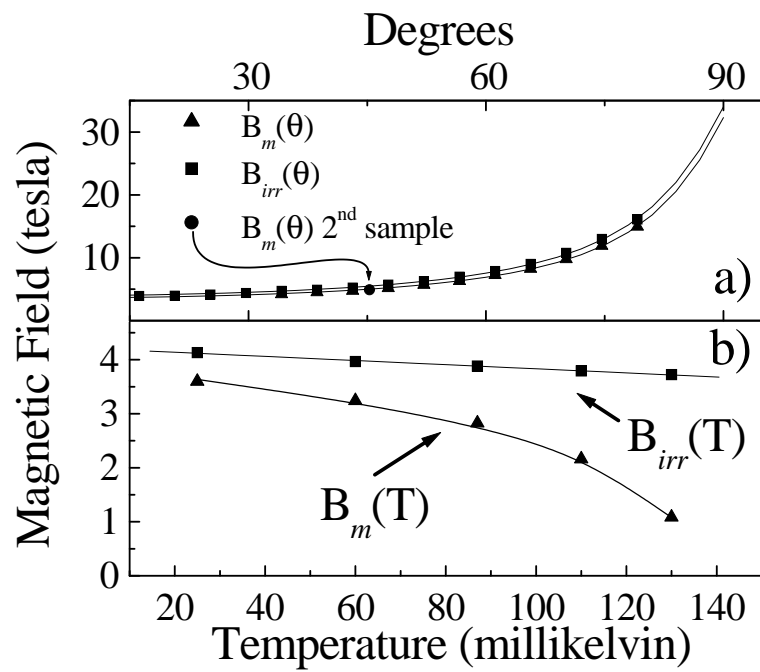


FIG. 4. Mola *et al.*